Chemistry & Biology, Vol. 10, 705–712, August, 2003, ©2003 Elsevier Science Ltd. All rights reserved. DOI 10.1016/S1074-5521(03)00159-5

The Structure of JNK3 in Complex with Small Molecule Inhibitors: Structural Basis for Potency and Selectivity

Giovanna Scapin,[1,*] Sangita B. Patel,[1] JeanMarie Lisnock,[2] Joseph W. Becker,[1] and Philip V. LoGrasso[3,4]

[1]Department of Medicinal Chemistry and
[2]Department of Metabolic Disorders
Merck Research Laboratories
P.O. Box 2000
Rahway, New Jersey 07065
[3]Department of Molecular Neuroscience
Merck Research Laboratories
3535 General Atomics Court
San Diego, California 92121

Summary

The c-Jun terminal kinases (JNKs) are members of the mitogen-activated protein (MAP) kinase family and regulate signal transduction in response to environmental stress. Activation of JNK3, a neuronal-specific isoform, has been associated with neurological damage, and as such, JNK3 may represent an attractive target for the treatment of neurological disorders. The MAP kinases share between 50% and 80% sequence identity. In order to obtain efficacious and safe compounds, it is necessary to address the issues of potency and selectivity. We report here four crystal structures of JNK3 in complex with three different classes of inhibitors. These structures provide a clear picture of the interactions that each class of compound made with the kinase. Knowledge of the atomic interactions involved in these diverse binding modes provides a platform for structure-guided modification of these compounds, or the de novo design of novel inhibitors that could satisfy the need for potency and selectivity.

Introduction

A growing body of evidence implicates the c-*jun* pathway, and particularly JNK3, in a variety of apoptotic neuronal cell death scenarios. Rat sympathetic neurons induced to die by nerve growth factor (NGF) deprivation can be protected by microinjection of neutralizing antibodies against c-*jun* [1] as well as by transfection of a dominant-negative form of c-*jun* [2]. More recently, the JNK pathway inhibitor CEP1347 has been shown to rescue rat embryonic motoneurons deprived of NGF or exposed to UV light or oxidative stress [3]. This compound also shows protection against MPTP-induced nigrostriatal dopaminergic neuronal loss in a mouse model of Parkinson's disease [4]. A similar result was seen by Xia et al. [5] who showed that gene transfer of the JNK inhibitor JIP-1 protects dopaminergic neurons against MPTP in a mouse model of Parkinson's disease. Direct evidence linking JNK3 to apoptotic neuronal cell death was reported by Yang et al. [6] who showed that JNK3-deficient mice were resistant to kanic acid-induced excitotoxicity and associated apoptotic cell death. Moreover, it has recently been shown that inhibitors of JNK3 are neuroprotective against NGF-withdrawal-induced cell death of rat sympathetic neurons [S.J. Harper, et al., 2002, FENS Forum, abstract; S.J. Harper, et al., 2002, Soc. Neurosci., abstract], as well as against 1-methyl-4-phenylpyridinium-induced cell death of dopaminergic neurons [J.G. Bilsland, et al., 2000, Fed. Eur. Neurosci., abstract]. Two other genes encoding JNKs, *Jnk1* and *Jnk2*, and at least ten different splicing isoforms have been identified in mammalian cells [7]. While JNK3 is selectively expressed in the brain and to a lesser extent in the heart and in the testis, JNK1 and JNK2 are widely expressed in a variety of tissues [7–9]. Studies with KO mice indicate that, although loss of the Jnk genes produces animals that are viable and show no gross differences from wild-type animals, some defects in T cell differentiation and proliferation, IL-2 production, and neuronal tube closure are associated with the loss of the Jnk1/2 genes [10, 11]. For these reasons, isoform selectivity is desirable for the development of safe compounds. Although the three isoforms share more than 90% sequence identity, each one has been shown to bind to the same substrates with different affinities [7], and small differences in primary sequence are present in their putative substrate binding site [12].

The design of selective kinase inhibitors has been a challenging problem because the great majority of known kinase inhibitors are ATP competitive and bind to a highly conserved ATP binding pocket [13–18]. The strong similarities among kinase ATP binding sites makes the development of selective inhibitors very difficult. Furthermore, the widespread use of purine-based cofactors by a variety of human proteins raises serious toxicity issues. Protein crystallography has provided a detailed view of the ATP binding site, revealing five distinct subsites with distinct chemical environments and local sequence features that afford an opportunity to develop highly specific kinase inhibitors. The subsites are: (1) a hydrophobic adenine binding site in which hydrogen bonds are made to nitrogen atoms of the adenine ring; (2) a hydrophilic sugar pocket that enfolds the ribose ring; (3) the solvent-exposed and hydrophilic phosphate binding region; (4) the hydrophobic region I, a pocket adjacent to N7 of the adenine ring; and (5) the hydrophobic region II, a slot opening to solvent (Figure 1) [14]. The two hydrophobic regions do not interact directly with bound ATP, but do contain residues that vary among kinases, and thus afford the medicinal chemist opportunities to develop selective inhibitors. As shown by several examples [14, 19–23], knowledge of the specific interactions made by an inhibitor in this site can lead to the design of highly selective compounds, despite the strong overall similarities among these proteins.

In this report we present the three-dimensional structures of JNK3 with four compounds, representing three

*Correspondence: giovanna_scapin@merck.com
[4]Present address: Avera Pharmaceuticals, 12730 High Bluff Drive, Suite 160, San Diego, California 92130.

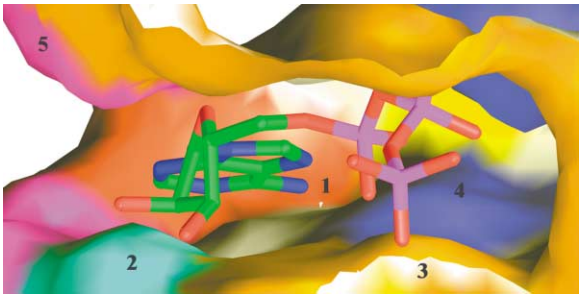

Figure 1. Schematic Representation of the ATP Binding Site in Kinases

ATP (in ball-and-sticks) interacts mainly with the linker/adenine binding region (1), the ribose binding region (2), and the phosphate binding region (3). The two hydrophobic regions I (4) and II (5) do not directly interact with ATP and contain residues that vary among kinases, thus providing possibilities for the development of selective inhibitors [17]. Figures 1, 2B, and 3–6 were made with RIBBONS [42].

distinct structural classes. Two of these compounds display significant selectivity in inhibition of p38 and JNK3 and two do not. Our results reveal the details of how these three classes of inhibitors interact with JNK3 as well as how the selective compounds distinguish that target from the closely related p38 kinase. We have found that: (1) inhibitors represented by the structural class of compound 3, and compound 4 (SP600125) are selective JNK inhibitors with potencies 20-fold and 265-fold greater than that for p38, respectively; (2) the increased potency of compound 2 relative to compound 1 against JNK3 is apparently due to interactions of its cyclohexyl ring with hydrophobic region II; (3) the selectivity of compound 3 for JNK3 versus p38 is probably due to the small, flat nature of this molecule and to its interaction with Gln155 in JNK3; and (4) the higher selectivity of compound 4 (SP600125) arises from its small size and flat shape that enable hydrophobic interactions that are not available in the larger, more hydrophilic p38 binding pocket. Taken together, these structures provide useful insights into the further development of MAP kinase family- and JNK isoform-selective inhibitors.

Results and Discussion

Novel JNK3 Inhibitors

The structures of four JNK3 inhibitors are given in Figure 2A. The crystal structures of JNK3 with each of these compounds were solved by X-ray diffraction analysis and refined to atomic resolution. Compounds 1 and 2 belong to the diarylimidazole family of MAP kinase inhibitors [24]. They are members of a family of MAP-kinase inhibitors that bind strongly to p38 [24], but not to the extracellular regulated kinase (ERK), and site-directed mutagenesis experiments on ERK have revealed many of the structural features that account for the inability of p38 inhibitors to bind to this kinase [25]. Compounds 1 and 2 are also potent JNK3 inhibitors with IC_{50}s of 7 and 1 nM, respectively (Figure 2A). They are efficacious in promoting neuronal survival of dopaminergic neurons exposed to MPP^+, and sympathetic neurons deprived of NGF [S.J. Harper, et al., 2002, FENS Forum, abstract; S.J. Harper, et al., 2002, Soc. Neurosci., abstract; J.G. Bilsland, et al., 2000, Fed. Eur. Neurosci., abstract], and thus hold promise as agents that may protect against neurodegeneration induced by multiple stimuli. They cannot be useful therapeutic agents, however, because both compounds are also potent p38 inhibitors (with IC_{50}s of 0.2 and 4 nM, respectively) and do not show any JNK isoform selectivity.

Compound 3 is a relatively weak JNK3 inhibitor (IC_{50} = 590 nM) but shows no p38 inhibition for concentrations up to 40 μM. Compound 4 (SP600125) [26] is a more potent JNK3 inhibitor (IC_{50} = 150 nM) than compound 3 and still shows no inhibition of p38 ($IC_{50} > 30$ μM) [26] (Figure 2A). Both compounds have been tested in our laboratory against a panel of protein kinases, and the results show that they are selective for JNK3 over a variety of other enzymes, including several protein tyrosine kinases (data not shown). Similar to the diarylimidazole inhibitors, compounds 3 and 4 show no JNK isoform selectivity.

Structure of JNK3:Compound 1

The structure of unphosphorylated JNK3 in complex with an ATP analog was originally reported in 1998 [27], and the structure reported here is substantially identical, with an rmsd on Cα atoms of 0.61 Å. The catalytic domain comprises an N-terminal domain spanning residues 45–149 and 379–400, and a C-terminal domain spanning residues 150–211 and 217–374. Residues 212–216 (part of the activation loop) were not visible in electron density maps and were not included in the model. As expected, compound 1 binds in the ATP binding site (Figure 2B). The bound inhibitor makes two hydrogen bond interactions with the protein, involving the main chain nitrogen and oxygen atoms of Met149 (3.0 and 3.2 Å, respectively) in the linker region. The hydrogen bond to the main chain nitrogen mimics the hydrogen bond made by ATP, and it has been shown in kinases in general to be essential for inhibitor binding [14, 28]; the presence of a second hydrogen bond has been directly related to the significant increases in potency observed for such compounds [19, 24]. The dichlorophenyl moiety is bound in hydrophobic region I [14] (Figure 1), a pocket lined by the side chains of Ala91, Lys93, Leu206, Ile124, Ile126, Leu144, and Met146, and the main chain atoms of Leu144-Met146 and Ala91-Lys93. Comparison of the JNK3:compound 1 complex to the JNK3:AMP-PNP complex (1JNK [27]) reveals only one notable conformational difference: the Met146 side chain adopts a different conformation, moving about 3 Å toward the back of the ATP binding site in order to accommodate the inhibitor. The cyclopropyl moiety of compound 1 is bound in the so-called hydrophobic pocket II [14] (Figure 1), within van der Waals distance of the side chains of Ile70, Ile148, Asn152, Gln155, and Val196, and the main chain atoms of residues 150–153. The piperidine ring of the inhibitor occupies the phosphate binding area, in noncovalent contact with the glycine-rich loop (Gly71-Val78). The piperidine ring is quite solvent exposed; several water molecules can be seen in this area, although only one (Wat673) interacts directly with the bound inhibitor.

A

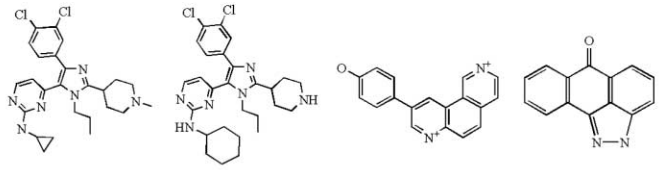

IC_{50}	Compound 1	Compound 2	Compound 3	Compound 4
JNK3	7.1 nM	1.6 nM	590 nM	150 nM
p38	0.078 nM	4.0 nM	> 40μM	> 30μM

B

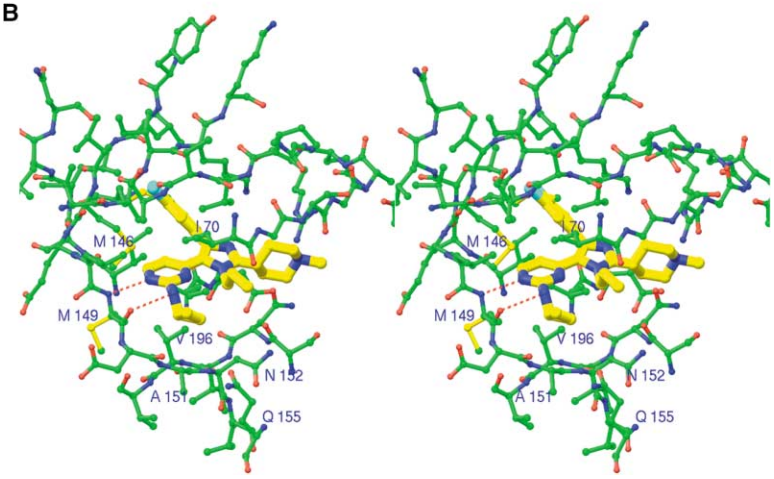

Figure 2. Chemical Structures and Binding Mode for JNK3 Inhibitors

(A) Chemical structure and IC_{50} for the four JNK3 inhibitors described in the text.

(B) Stereo view of compound 1 bound to the ATP binding site of JNK3. The hydrogen bond interactions made with the main chain of Met149 are shown as red dotted lines. Other key active site residues are noted.

Comparison of the structures of the JNK3:compound 1 complex and of p38 in complex with an analog of compound 1 [29] (PDB code 1OUK) reveals regions of similarity and diversity in the ATP binding pocket that may help in the design of compounds selective for either enzyme. JNK3 and p38 share 51% identity in primary sequence. Their three-dimensional structures are also extremely similar, although the relative orientations of their N- and C-terminal domains are different, as previously observed [27]. Despite the different orientation, the structures of the individual domains are quite similar, with rmsds of 1.28 and 1.45 Å for the N- and C-terminal domains, respectively. Before comparing the structures in detail, however, it is worth considering whether the different domain orientation may be an artifact caused by the fact that the JNK3 structures were obtained in presence of ATP analogs (displaced during soaks by the higher affinity ligands), while the p38 structure used in the comparison was not. Additional reservations arise because the p38 complex was obtained by soaking the inhibitor into a crystal of the apoprotein, and this procedure might have introduced biases (because of crystal lattice contacts, or preorganized structures) that could partially obscure the real interactions between a protein and its ligand. Two key observations suggest that these issues do not preclude meaningful comparisons of the available JNK3 and p38 structures. First, although there are no structures available for apo-JNK3, several structures are available for p38 complexes, and they show that the structures of the complexed and uncomplexed enzyme are essentially identical [19, 29. 30]. Second, we now have cocrystals of p38 with other inhibitors (G.S., unpublished data), which show that the p38 structure does not change dramatically upon inhibitor binding. In addition, the structure of the JNK3 complex with compound 3 reported here was obtained via a cocrystallization experiment, and it is essentially identical to the three structures obtained by soaking. It is then reasonable to expect that the relative shape and size of the binding cavities will be maintained upon ligand binding, thus suggesting that it is meaningful to examine these structures in order to understand the structural bases of selectivity.

Figure 3 is a comparison between the JNK3 and p38 ATP binding sites. Panel A is a schematic view of compound 1 bound to JNK3; highlighted in the figure, and listed to the right, are the residues in or near the ATP binding site that are different between JNK3 and p38. Four of the six nonconserved residues (between JNK3 and p38) are smaller in p38, meaning that p38 can accommodate larger inhibitors that would not be effective against JNK3. In addition, the different relative orientations of the N- and C-terminal domains in the two enzymes make the ATP binding pocket wider in p38 than in JNK3 (Figures 3B and 3C). Indeed, a number of site-directed mutagenesis studies on p38 where Thr106 in p38 was mutated to the corresponding residue in JNK3 (Met) or ERK2 (Gln) have shown that this residue contributes significantly to the selectivity of many p38 inhibitors [19, 30, 31]. This analysis suggests that small, flat inhibitors that do not reach into pockets conferring p38 specificity, but do rely mostly on hydrophobic interactions

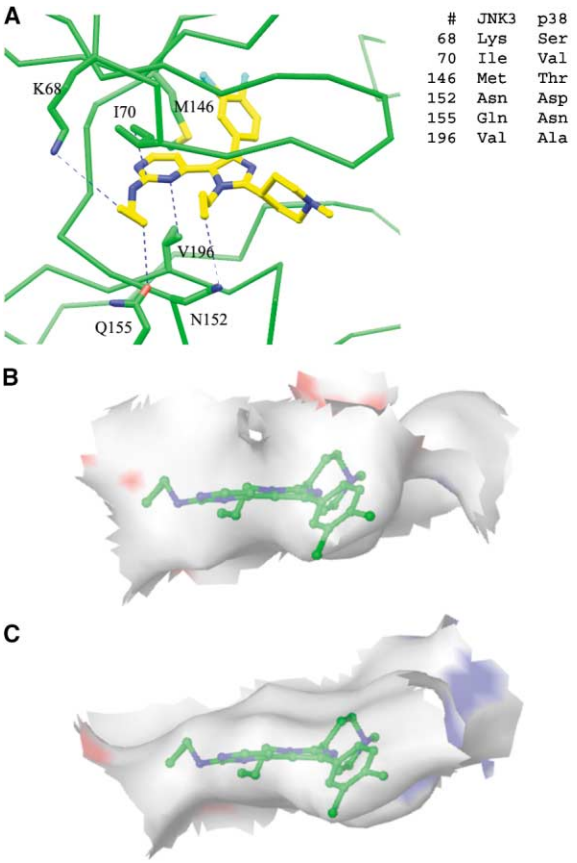

Figure 3. Comparison of the ATP Binding Sites in JNK3 and p38

(A) Schematic view of compound 1 bound to JNK3. Possible interactions are indicated by the dashed lines. Highlighted in the figure, and listed to the right, are the residues in or near the ATP binding site that are different between JNK3 and p38.

(B) Surface representation of the ATP binding site in p38.

(C) Surface representation of the ATP binding site in JNK3.

for binding, would be JNK3 specific. This idea is borne out by compounds 3 and 4 (below).

Structure of JNK3:Compound 2

Compound 2 binds to JNK3 essentially as compound 1 does. This compound is 7-fold more potent than compound 1; the increase in potency is probably due to the replacement of the cyclopropyl ring with a cyclohexyl ring. The larger ring optimizes interactions with the side chains of Ile70 (4.2 Å in complex 2 versus 5.4 Å in complex 1), Ile148 (5.1 versus 5.7 Å), Asn152 (4.0 versus 5.4 Å) and Gln155 (3.4 versus 4.3 Å). This last contact also suggests that introducing a polar contact by, for example, using a piperidine in this position may improve potency. Gln155 corresponds to Asn115 in p38, and, as discussed below, the smaller residue in p38 may be useful in obtaining discrimination between JNK3 and p38. Comparison between the structures of compound 1- and compound 2-bound JNK3 suggests that it could be possible to target selectivity by modifying this class of compounds to take advantage of the small differences between the two enzymes without a major loss in potency.

Although compound 2 belongs to the same class of inhibitors as compound 1, and thus shares its liabilities, the crystal structure of JNK3 in complex with compound 2 reveals a striking and possibly useful new feature that could be used to discriminate among the different JNK isoforms. As mentioned before, the structure of compound 2 bound to JNK3 was obtained by overnight soaking of the compound into crystals grown in AMP-PCP. During refinement, it was clear that in both 2Fo-Fc and Fo-Fc Fourier maps there was a continuous residual positive electron density near the bound inhibitor that could not be attributed to protein or inhibitor atoms. The electron density was fitted as AMP-PCP, complexed to the N-4-piperydil nitrogen of the compound (Figure 4). The AMP-PCP is not in the canonical ATP binding site, as found in the 1JNK structure, which is occupied by the inhibitor. Rather, the AMP-PCP molecule is hydrogen bonded to the N-4-piperidyl nitrogen of compound 2, and extends toward the putative protein binding site [9], where it makes several hydrogen bond interactions to protein and solvent atoms. The adenine interacts with Glu255 and Ile261 in the putative substrate binding domain (Ile246-Tyr268), which is the region that displays the greatest diversity among JNKs isoforms. This unusual complex suggests a means of designing bidentate inhibitors that extend from the ATP binding pocket toward the substrate binding area, thus enabling the design of very selective kinase inhibitors [32] that may also address the issue of isoform selectivity.

Structure of JNK3:Compound 3

Compound 3 (Figure 2A) is a 590 nM JNK inhibitor, with no detectable p38 activity up to 40 μM. The compound was discovered by screening the Merck compound collection, and has a structure strikingly different from most previously described kinase inhibitors. Although a relatively weak inhibitor, compound 3 is small and thus suitable for chemical modifications that may improve both potency and selectivity, and those modifications can be guided by our results. Crystals of this compound were obtained by cocrystallization, under conditions similar to that of the AMP-PCP complex originally reported. Compound 3 is bound in a portion of the ATP binding site (Figure 5) comprising the adenine binding pocket and hydrophobic region II. The inhibitor makes four hydrogen bonds: one with the linker region (main chain nitrogen of Met149, 2.5 Å), two with the side chain of Gln155 (2.6 and 3.0 Å, respectively), and one with the main chain nitrogen of Gln75 (2.9 Å). Gln155 corresponds to Asn115 in p38, and given the different orientation of the two kinase lobes and the smaller size of asparagine, its side chain would be about 5.8 Å away from the ligand in a comparable p38 complex. There are no other residues nearby in p38 that could provide an interaction similar to that seen in JNK3; Gln155 may thus play a critical role in the selectivity of compound 3 for JNK3 over p38. Another reason for the observed selectivity is that compound 3 is a small, flat, hydrophobic molecule that, as suggested before, probably binds better to the smaller JNK3 site than to the wider and more solvent-exposed p38 cavity.

The interaction with the main chain nitrogen of Gln75

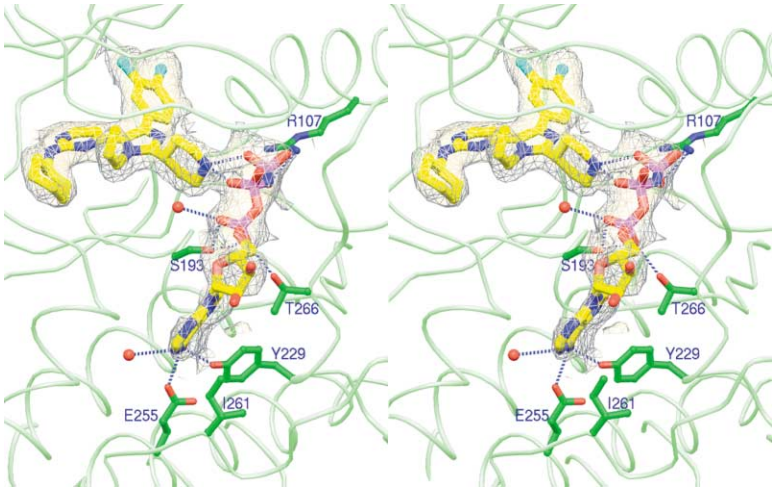

Figure 4. Stereoview of the ATP Binding Site in the JNK3:Compound 2 Complex, Showing the Location of the AMP-PCP Molecule that Was Found in the Structure

The 2Fo-Fc electron density (contoured at 1.0 s) for both compound 2 and AMP-PCP is also displayed. The AMP-PCP was hydrogen bonded to the N-4-piperidyl nitrogen of compound 2, and extended toward the putative substrate binding domain (I246-Y268) [9].

is made possible by a dramatic change in the conformation of the Gly-rich loop, the flap that in all kinases covers the phosphate binding region of the ATP binding site. Figure 5A shows the Cα trace of JNK3:compound 1 superimposed on the compound 3 complex; a portion of the glycine-rich loop spanning residues Ile70-Ile77 bends almost 90° away from the position observed in complex 1. This region of the protein kinases is very flexible, and a ligand-induced conformational change similar to the one observed here has been reported

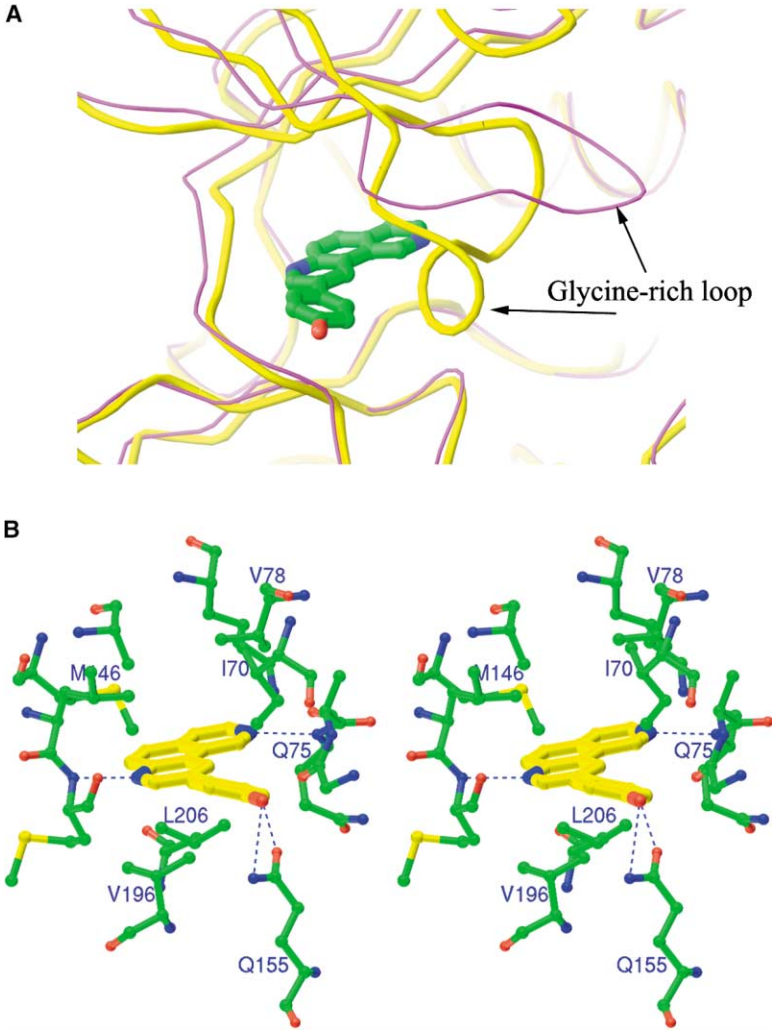

Figure 5. Binding of Compound 3 to JNK3

(A) Overlay of the Cα traces of JNK3:compound 1 (magenta) and JNK3:compound 3 complexes (yellow) in the region of the glycine-rich loop (G71-V78). The conformational change observed for residues Ile70–Ile77 was ligand induced.

(B) Close-up of the compound 3 binding site; hydrogen bond interactions with protein atoms are shown as blue dotted lines.

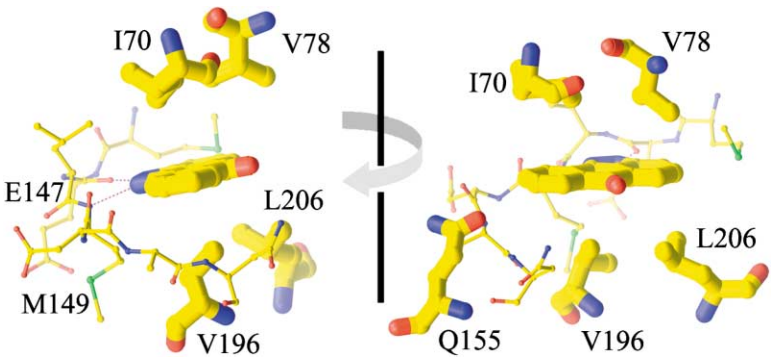

Figure 6. Close-Up of the Binding Site in the JNK3:Compound 4 Complex: the Two Panels Represent Two Views 90° Apart

The residues that are not conserved in p38 and thus responsible for the selectivity for JNK3 over p38 displayed by this compound are shown as thick ball-and-stick.

for the tyrosine kinase domain of the fibroblast growth factor receptor 1 in complex with SU5402 [33]. The sequences of p38 and JNK3 are basically identical in the Gly-rich loop, with the only difference being a Gln to Tyr mutation at position 75 (residue 35 in p38). The inhibitor interacts only with the main chain atoms of this residue, so they should not be affected by the difference in sequence. In addition, a similar loop movement has been observed in p38 upon binding of one of our compounds (G.S., unpublished data), suggesting that this loop movement is not a primary cause of the selectivity of compound 3 for JNK3 over p38.

Structure of JNK3:Compound 4 (SP 600125)

Compounds in this class were originally identified as JNK3 inhibitors by Signal Pharmaceutical (now part of Celgene); we identified compound 4 (SP600125) by screening of our compound collection. Compound 4 inhibits JNK1 and -2 with an IC_{50} of 110 nM, and JNK3 with an IC_{50} of 150 nM, but is much less active on p38, with an $IC_{50} > 30\ \mu M$ [26], which makes it, to our knowledge, the most selective JNK3 inhibitor available. As with compounds 1 and 2, the complex of JNK3 with compound 4 was obtained by soaking an AMP-PNP-containing crystal overnight in a 1 mM solution of inhibitor. The electron density for the inhibitor was quite clear in the ATP binding site. Compound 4 makes hydrogen bonds with the carbonyl oxygen of Glu147 (2.8 Å) and the main chain nitrogen of Met149 (2.8 Å) in the linker region (Figure 6). These two interactions are similar to those formed by compounds 1 and 2 and may explain why the relatively small compound 4 is nevertheless quite potent. The selectivity for JNK3 over p38 likely arises because the inhibitor is, like compound 3, within van der Waals distance from several residues that line the ATP binding site (4.1 Å from Ile70, 4.3 Å from Val78, 4.2 Å from Ile124, 3.8 Å from Val196, and 3.8 Å from Leu206, Figure 6). Most of these residues are not conserved in p38, and even if conserved would be farther from the inhibitor, i.e., Ile70 corresponds to a valine, whose side chain would be 5.2 Å from the bound inhibitor, and Val196 to an alanine (6.5 Å away). Val78, Ile124, and Leu206 are conserved, but their distance from the inhibitor would be increased to 4.5, 4.8, and 4.5 Å, respectively. This analysis indicates that compound 4, which is small, flat, hydrophobic, and relies largely on hydrophobic interactions for binding, finds in JNK3 an optimized environment, while the larger cavity in p38 cannot fully form these productive hydrophobic interactions (Figures 3A, 3B, and 6). In addition, based on the structure of the JNK3:compound 3 complex, it is apparent that suitable modifications of compound 4 could allow for interactions with Gln155 with possible increase in both potency and selectivity.

Significance

The c-Jun terminal kinases (JNKs) are members of the MAP kinase family and regulate signal transduction in response to environmental stress. Activation of JNK3, a neuronal-specific isoform, has been associated with neurological damage, and as such, JNK3 may represent an attractive target for the treatment of neurological disorders. Although the discovery of selective kinase inhibitors has been a challenging problem because the great majority of known kinase inhibitors bind to the highly conserved ATP binding pocket, knowledge of the specific interactions made by a compound in this site can lead to the design of highly selective compounds. In this report we present the three-dimensional structures of JNK3 in complex with four compounds, representing three distinct structural classes. The compounds range in potency between 1 and 590 nM, and display different selectivity in inhibition of p38 and JNK3. Our results reveal the details of how these three classes of inhibitors interact with JNK3 as well as how the selective compounds distinguish this target from the closely related p38 kinase. The structures show that potency can be achieved by specific interactions with residues of the ATP binding site. In addition, we show that small, flat, hydrophobic molecules interact preferentially with JNK3 and afford considerable selectivity over p38. Knowledge of the atomic interactions revealed by our studies may provide a platform for the further development of MAP kinase family- and JNK isoform-selective inhibitors that could satisfy the need for potency against JNK3 and selectivity against other protein kinases.

Experimental Procedures

Cloning and Expression

JNK3 was cloned and expressed as described in Lisnock et al. [34]

Purification and Crystallization

JNK3 was purified following the published protocol [27]. The protein was initially stored in 25 mM HEPES, pH 7.0, 2.5% glycerol, 50 mM

Table 1. Statistics for the Data Sets Used to Solve the Structures of the Complexes Described in the Paper and Final Statistics for the Refined Models

	Compound 1[a]	Compound 2[b]	Compound 3[a]	Compound 4[b]
UCP (Å)	a = 53.07 Å b = 71.34 Å c = 107.17 Å	a = 50.95 Å b = 71.53 Å c = 106.00 Å	a = 62.40 Å b = 62.38 Å c = 98.12 Å	a = 48.21 Å b = 73.09 Å c = 106.04 Å
Resolution range (Å)	22.0–2.2 (2.3–2.2)	17.0–2.2 (2.3–2.2)	25.0–2.7 (2.8–2.7)	30.0–2.5 (2.6–2.5)
No. reflections	21,026 (3,431)	19,487 (1,594)	10,987 (1,668)	12,783 (1,086)
% of possible	98.6 (98.5)	95.6 (80.1)	100 (100)	94.4 (81.1)
Redundancy	6.1 (5.8)	7.8 (7.6)	5.9 (6.2)	5.5 (5.8)
I/σI	8.6 (2.4)	10.0 (3.0)	5.7 (1.3)	7.0 (1.4)
R_{sym}	5.9 (19.7)	6.1 (17.7)	12.3 (45.4)	7.2 (34.1)
Refinement Statistics				
Resolution range (Å)	22.0–2.2	17.0–2.2	25.0–2.7	30.0–2.5
No. of reflections[c]	21,014	19,386	10,496	12,750
% of possible	98.6	95.7	95.5	94.3
R_{free}/R	26.6/22.8	26.2/22.8	28.5/21.8	28.2/21.8
Rmsd bond length/angle	0.012/1.47	0.011/1.4	0.011/1.42	0.011/1.24
No. of protein atoms	2777	2805	2752	2787
No. of solvent atoms	197	55	63	101
No. of ligand atoms	33	66	22	19

Numbers in parentheses refer to last resolution shell.
[a] Integration, scaling, and merging of the data were done using X-GEN [40].
[b] Integration, scaling, and merging of the data were done using HKL2000 [41].
[c] No σ cut off was used during refinement.

NaCl, 10 mM DTT, but dynamic light scattering analysis indicated that the protein was severely polydisperse. Several buffer conditions were then tried in order to obtain a monodisperse solution of protein: the best buffer was 20 mM HEPES, pH 7.0, 50 mM NaCl, 0.02% n-octyl-glucopyranoside, 5 mM TCEP. Crystals of the JNK3:AMP-PCP complex were obtained by vapor diffusion in hanging drops: the enzyme (10 mg/ml protein in buffer containing 1 mM AMP-PCP and 2 mM $MgCl_2$) was equilibrated at room temperature against a reservoir containing 20% PEG MME 550, 10% ethylene glycol in 0.1 M HEPES, pH 7.3. Crystals of the compound 1, 2, and 4 complexes were obtained by soaking the AMP-PCP-containing crystals overnight in 1 mM compound in mother liquor. Crystals of the compound 3 complex were obtained by hanging-drop cocrystallization under very similar conditions (19% PEG MME 550, 10% ethylene glycol, 0.1 M HEPES, pH 7.3), after incubating the enzyme with a 2-fold excess of inhibitor for 1.5 hr in ice.

Data Collection and Structure Solution and Refinement

All data sets were collected on single crystals, vitrified at 100 K, using synchrotron radiation at beamline 17-ID in the facilities of the Industrial Macromolecular Crystallography Association Collaborative Access Team (IMCA-CAT) at the Advanced Photon Source. The soaked crystals are isomorphous with those previously reported [27]; they belong to the orthorhombic space group $P2_12_12_1$, with unit cell parameters approximately a = 50 Å, b = 70 Å, c = 105 Å (Table 1) and one molecule per asymmetric unit. The crystals of the compound 3 complex are also orthorhombic, $P2_12_12_1$, but with unit cell parameters a = 62.4 Å, b = 62.4 Å, c = 98.1 Å. Table 1 reports the final statistics on the data. For the compound 1, 2, and 4 complexes, initial difference Fourier electron density maps were used to locate the bound ligand using a starting model the coordinates of the AMP-PNP:JNK3 complex (PDB code 1JNK), without waters or bound ligand. Refinement was carried out alternating cycles of manual rebuilding using the graphic software O [35, 36] and computer-based refinement using CNX [37]. Typically, two cycles of torsion angle dynamics refinement [38], followed by positional and temperature factor refinement were run in each cycle. Bulk solvent correction was applied throughout the entire refinement. For the compound 3 complex, the structure was initially solved by molecular replacement using AMoRe [39] and the structure of JNK3:compound 1 complex (without waters and ligand) as search model. The final solution had a correlation coefficient of 46.6% and R factor of 35.6% for data between 8 and 4 Å. Analysis of crystal packing showed that there were some severe steric clashes involving residues 210–227 and 365–384. These residues were omitted during the initial refinement, and slowly built back into the available density. Residues 70–76 (of the Gly-rich loop) were also omitted and rebuilt at a later stage. Volunteer electron density for the bound inhibitor was available since the initial map, but compound 3 was included in the model at a much later stage. The refinement of this complex was carried out essentially as for the previous complexes. Table 1 summarizes the final statistics for all four complexes.

Acknowledgments

We thank the staff at the facilities at the Industrial Macromolecular Crystallography Association Collaborative Access Team (IMCA-CAT) for help during data collection. The facilities at IMCA-CAT are supported by the companies of the Industrial Macromolecular Crystallography Association through a contract with Illinois Institute of Technology (IIT), executed through IIT's Center for Synchrotron Radiation Research and Instrumentation. Use of the Advanced Photon Source was supported by the U.S. Department of Energy, Basic Energy Sciences, Office of Science, under Contract No. W-31-109-Eng-38.

Received: April 30, 2003
Revised: June 16, 2003
Accepted: June 23, 2003
Published: August 22, 2003

References

1. Estus, S., Zaks, W.J., Freeman, R.S., Gruda, M., Bravo, R., and Johnson, E.M. (1994). Altered gene expression in neurons during programmed cell death: identification of c-jun as necessary for neuronal apoptosis. J. Cell Biol. *127*, 1717–1727.
2. Ham, J., Babij, C., Whitfield, J., Pfarr, C.M., Lallemand, D., Yaniv, M., and Rubin, L.L. (1995). A c-Jun dominant negative mutant protects sympathetic neurons against programmed cell death. Neuron *14*, 927–939.
3. Maroney, A.C., Finn, J.P., Bozyczko-Coyne, D., O'Kane, T.M., Neff, N.T., Tolkovsky, A.M., Park, D.S., Yan, C.Y.I., Troy, C.M., and Greene, L.A. (1999). CEP-1347 (KT7515), an inhibitor of

JNK activation, rescues sympathetic neurons and neuronally differentiated PC12 cells from death evoked by three distinct insults. J. Neurochem. *63*, 1901–1912.

4. Saporito, M.S., Brown, E.M., Miller, M.S., and Carswell, S. (1999). CEP-1347/KT-7515, an inhibitor of c-jun N-terminal kinase activation, attenuates the 1-methyl-4-phenyl tetrahydropyridine-mediated loss of nigrostriatal dopaminergic neurons in vivo. J. Pharmacol. Exp. Ther. *288*, 421–427.
5. Xia, X.G., Harding, T., Weller, M., Bieneman, A., Uney, J.B., and Schulz, J.B. (2001). Gene transfer of the JNK interacting protein-1 protects dopaminergic neurons in the MPTP model of Parkinson's disease. Proc. Natl. Acad. Sci. USA *98*, 10433–10438.
6. Yang, D.D., Kuan, C.Y., Whitmarsh, A.J., Rincon, M., Zheng, T.S., Davis, R.J., Rakic, P., and Flavell, R.A. (1997). Absence of excitotoxicity-induced apoptosis in the hippocampus of mice lacking the Jnk3 gene. Nature *389*, 865–870.
7. Gupta, S., Barrett, T., Whitmarsh, A.J., Cavanagh, J., Sluss, H.K., Derijard, B., and Davis, R.J. (1996). Selective interaction of JNK protein kinase isoforms with transcription factors. EMBO J. *15*, 2760–2770.
8. Mohit, A.A., Martin, J.H., and Miller, C.A. (1995). p493F12 kinase: a novel MAP kinase expressed in a subset of neurons in the human nervous system. Neuron *14*, 67–78.
9. Martin, J.H., Mohit, A.A., and Miller, C.A. (1996). Developmental expression in the mouse nervous system of the p493F12 SAP kinase. Brain Res. Mol. Brain Res. *35*, 47–57.
10. Chang, L., and Karin, M. (2001). Mammalian MAP kinase signalling cascades. Nature *410*, 37–40.
11. Harper, S.J., and LoGrasso, P. (2001). Inhibitors of the JNK signaling pathway. Drugs Future *26*, 957–973.
12. Kallunki, T., Su, B., Tsigelny, I., Sluss, H.K., Derijard, B., Moore, G., Davis, R., and Karin, M. (1994). JNK2 contains a specificity-determining region responsible for efficient c-Jun binding and phosphorylation. Genes Dev. *8*, 2996–3007.
13. McMahon, G., Sun, L., Liang, C., and Tang, C. (1998). Protein kinase inhibitors: structural determinants for target specificity. Curr. Opin. Drug Discov. Dev. *1*, 131–146.
14. Toledo, L.M., Lydon, N.B., and Elbaum, D. (1999). The structure-based design of ATP-site directed protein kinases inhibitors. Curr. Med. Chem. *6*, 775–805.
15. Garcia-Echeverria, C., Traxler, P., and Evans, D.B. (2000). ATP site-directed competitive and irreversible inhibitors of protein kinases. Med. Res. Rev. *20*, 28–57.
16. Sausville, E.A. (2000). Protein kinase antagonists: interim challenges and issues. Anticancer Drug Des. *15*, 1–3.
17. Dumas, J. (2001). Protein kinase inhibitors: emerging pharmacophores 1997–2000. Expert Opin. Ther. Pat. *11*, 405–429.
18. Bridges, A.I. (2001). Chemical inhibitors of protein kinases. Chem. Rev. *101*, 2541–2572.
19. Wang, Z., Canagarajah, B.J., Boehm, J.C., Kassisa, S., Cobb, M.H., Young, P.R., Abdel-Meguid, S., Adams, J.L., and Goldsmith, E.J. (1998). Structural basis of inhibitor selectivity in MAP kinases. Structure *6*, 1117–1128.
20. Zhu, X., Kim, J.L., Newcomb, J.R., Rose, P.E., Stover, D.R., Toledo, L.M., Zhao, H., and Morgenstern, K.A. (1999). Structural analysis of the lymphocyte-specific kinase Lck in complex with non-selective and Src family selective kinase inhibitors. Structure *7*, 651–661.
21. Schindler, T., Bornmann, W., Pellicena, P., Miller, W.T., Clarkson, B., and Kuriyan, J. (2000). Structural mechanism for STI-571 inhibition of abelson tyrosine kinase. Science *289*, 1938–1942.
22. Davies, T.G., Pratt, D.J., Endicott, J.A., Johnson, L.N., and Noble, M.E.M. (2002). Structure-based design of cyclin-dependent kinase inhibitors. Pharmacol. Ther. *93*, 125–133.
23. Scapin, G. (2002). Structural biology in drug design: selective protein kinase inhibitors. Drug Discov. Today *7*, 601–611.
24. Liverton, N.J., Butcher, J.W., Claiborne, C.F., Claremon, D.A., Libby, B.E., Nguyen, K.T., Pitzenberger, S.M., Selnick, H.G., Smith, G.R., Tebben, A., et al. (1999). Design and synthesis of potent, selective, and orally bioavailable tetrasubstituted imidazole inhibitors of p38 mitogen-activated protein kinase. J. Med. Chem. *42*, 2180–2190.
25. Eyers, P.A., Craxton, M., Morrice, N., Cohen, P., and Goedert, M. (1998). Conversion of SB 203580-insensitive MAP kinase family members to drug-sensitive forms by a single amino-acid substitution. Chem. Biol. *5*, 321–328.
26. Han, Z., Boyle, D.L., Chang, L., Bennett, B., Karin, M., Yang, L., Manning, A.M., and Firestein, G.S. (2001). c-jun N-terminal kinase is required for metalloproteinase expression and joint destruction in inflammatory arthritis. J. Clin. Invest. *108*, 73–81.
27. Xie, X., Gu, Y., Fox, T., Coll, J.T., Fleming, M.A., Markland, W., Caron, P.R., Wilson, K.P., and Su, M.S. (1998). Crystal structure of JNK3: a kinase implicated in neuronal apoptosis. Structure *6*, 983–991.
28. Boehm, J.C., and Adams, J.L. (2000). New inhibitors of p38 kinase. Expert Opin. Ther. Pat. *10*, 25–37.
29. Fitzgerald, C.E., Patel, S.B., Becker, J.W., Cameron, P.M., Zaller, D., Pikounis, V.B., O'Keefe, S.J., and Scapin, G. (2003). Structural basis for p38alpha MAP kinase quinazolinone and pyridol-pyrimidine inhibitor specificity. Nat. Struct. Biol., in press.
30. Wilson, K.P., McCaffrey, P.G., Hsiao, K., Pazhanisamy, S., Galullo, V., Bemis, G.W., Fitzgibbon, M.J., Caron, P.R., Murcko, M.A., and Su, M.S.S. (1997). The structural basis for the specificity of pyridinylimidazole inhibitors of p38 MAP kinase. Chem. Biol. *4*, 423–431.
31. Lisnock, J.M., Tebben, A., Frantz, B., O'Neill, E.A., Croft, G., O'Keefe, S.J., Li, B., Hacker, C., de Laszlo, S., Smith, A., et al. (1998). Molecular basis for p38 protein kinase inhibitor specificity. Biochemistry *37*, 16573–16581.
32. Parang, K., Till, J.H., Ablooglu, A.J., Kohanski, R.A., Hubbard, S.R., and Cole, P.A. (2001). Mechanism-based design of a protein kinase inhibitor. Nat. Struct. Biol. *8*, 37–41.
33. Mohammadi, M., McMahon, G., Sun, L., Tang, C., Hirth, P., Yeh, B.K., Hubbard, S.R., and Schlessinger, J. (1997). Structures of the tyrosine kinase domain of fibroblast growth factor receptor in complex with inhibitors. Science *276*, 955–960.
34. Lisnock, J., Griffin, P., Calaycay, J., Frantz, B., Parsons, J., O'Keefe, S.J., and LoGrasso, P. (2000). Activation of JNK3 alpha 1 requires both MKK4 and MKK7: kinetic characterization of in vitro phosphorylated JNK3 alpha 1. Biochemistry *39*, 3141–3148.
35. Jones, A.T., Zuo, J.Y., Cowan, S.W., and Kjeldgaard, M. (1991). Improved methods for building protein models in electron density maps and the location of errors in these models. Acta Crystallogr. A *47*, 110–119.
36. Jones, A.T., and Kjeldgaard, M. (1997). Electron-density map interpretation. Methods Enzymol. *277*, 173–208.
37. Brünger, A.T., Adams, P.D., Clore, G.M., DeLano, W.L., Gros, P., Grosse-Kunstleve, R.W., Jiang, J.-S., Kuszewski, J., Nilges, M., Pannu, N.S., et al. (1998). Crystallography & NMR system: a new software suite for macromolecular structure determination. Acta Crystallogr. D *54*, 905–921.
38. Rice, L.M., and Brunger, A.T. (1994). Torsion angle dynamics: reduced variable conformational sampling enhances crystallographic structure refinement. Proteins *19*, 277–290.
39. Navaza, J. (1994). AMoRe: an automated package for molecular replacement. Acta Crystallogr. A *50*, 157–163.
40. Howard, A.J. (2001). Data processing in Macromolecular Crystallography. In Crystallographic Computing 7: Proceedings from the Macromolecular Crystallographic Computing School, 1996, E.P.E. Bourne and K.D. Watenpaugh, eds. (Oxford, UK: Oxford University Press), pp. 150–165.
41. Otwinowski, Z., and Minor, W. (1997). Processing of x-ray diffraction data collected in oscillation mode. Methods Enzymol. *276*, 307–326.
42. Carson, M. (1997). Ribbons. Methods Enzymol. *277*, 493–505.

Accession Numbers

Coordinates and structure factors for complexes 1–4 have been deposited in the Protein Data Bank with accession codes 1PMN, 1PMQ, 1PMU, and 1PMV for immediate release upon publication.